Mode-Group Division Multiplexing: transmission, node architecture, and provisioning

P. Boffi, N. Sambo, P. Martelli, P. Parolari, A. Gatto, F. Cugini, P. Castoldi

Abstract—**Few Mode Fibers (FMF) and Space Division Multiplexing (SDM) are an attractive solution to offer high capacity in optical networks. Although transmission along FMF presents several issues mainly due to the cross-talk among modes, the use of Multiple Input Multiple Output (MIMO) coherent receivers permits to limit the impact of such physical impairment. However, the complexity of MIMO is not negligible (especially with a large number of modes) and the spatial modes must cover the same path, thus limiting network flexibility, e.g. routing modes along different paths is not admitted.**

In this paper we exploit the concept of Mode-Group Division Multiplexing (MGDM) and we investigate the network architecture and provisioning supporting MGDM. Modes are divided in groups: the modes within a group are co-routed and received with a reduced-complexity MIMO receiver, while the different groups can be routed along different paths. Different node architectures supporting MGDM are presented taking in account state-of-the-art components and devices, even commercially available on the market. A quality of transmission (QoT) model is also presented accounting to the inter mode group crosstalk, that cannot be neglected in the reach evaluation. QoT is exploited by a proposed connection provisioning scheme for MGDM. Simulations are carried out in metro/rural network scenarios with different link span lengths. Simulations show high throughput increase while limiting the complexity of receivers.

Index Terms— **SDM, multi-mode, multi-core, FMF.**

I. INTRODUCTION

S PACE DIVISION MULTIPLEXING (SDM) over few-mode fibers (FMFs) has been demonstrated as an attractive solution to increase the whole transported capacity in optical networks [1]. Even if significant inter-modal crosstalk (IMXT) is accumulated during FMF propagation with respect to the employment of multi-core fibers (MCFs), the use of full digital MIMO allows to demultiplex all the received spatial modes [2]. This complex DSP implementation reduces the limitations due to in-band IMXT, but all the spatial modes must cover the same physical path [3] to be processed together at the receiver after coherent detection, permitting just point-to-point transmission, thus reducing the flexibility of networking. In any case, all the modes must be accessible in each node receiver during the connection to allow full MIMO processing, even if the modes contain services with different destinations [4].

An advantage in optical networks would be the exploitation of mode-division multiplexing (MDM) also for mode routing, enabling all-optical mode switching/aggregation and handling at the node level both in spectrum and space, such as it is achieved in case of SDM based on MCFs [5-8].

In the context of SDM networks, several papers already proposed spectrum routing and space-dimension assignment strategies for SDM [9-14]. In [15,16], node architectures enabling independent, joint, and fractional switching of spatial dimensions are proposed, reviewed, and compared. The authors propose reconfigurable optical add and drop multiplexers (ROADMs) suitable for uncoupled spatial dimensions, as offered by parallel single mode fibers (SMFs) and fibers with uncoupled cores where individual spatial and wavelength channels can be routed independently. In [17], regarding MCFs, a variety of node architectures based on core selective switches is proposed. In [18], spatial bypass is introduced for parallel SMFs or MCFs. Several SDM approaches have been also compared (parallel fibers, MCF, FMF). In [19], the authors performed a techno-economic analysis to identify the cost reduction of the SDM schemes compared to conventional approaches based on parallel-fiber systems. In [20], assuming that SDM integration of amplifiers and transponders has been shown to drive cost savings, additional cost benefits are examined for multi-core fibers. In [21], the author assesses that to fully exploit already deployed fibers, SDM networks will have to operate over a mixed infrastructure of parallel deployed single-mode fiber — which, when exhausted, may gradually be replaced by new fiber technologies (e.g., multi mode). Regarding FMF-based SDM optical networks, in order to enable more flexibility supporting the switching/aggregation in space by using the modes, mode-group division multiplexing (MGDM) [22,23] can be adopted. Indeed, in a FMF, independent mode groups can be identified, characterized by theoretically weak or even negligible IMXT between the spatial modes belonging to different groups, also called inter-mode group crosstalk (IGXT). On the contrary, the spatial modes of the same group, strongly coupled, constitute a single modal super-channel. MGDM solution does not only allow to apply FMF-based SDM in mesh networks

(independently managing the different mode groups), but also reduces the complexity of the MIMO at the receiver with respect to the full MIMO approach.

MGDM appears very attractive in terms of network provisioning and flexibility [24] to cope with the enormous bandwidth demand increase: the main issue of the exploitation of MGDM in a mesh network remains the real practical implementation of a network node able to handle both the spectrum and the modes. Recently, different spatial mode multiplexers/demultiplexers (MUXs/DEMUXs) have been introduced in the market [25], with the possibility to all-optically multiplex/demultiplex spatial modes. However, these mode MUXs/DEMUXs are just a possible building-block of node architectures able to support MGDM which are still to be developed.

In this paper, we analyze MGDM capabilities for dynamic provisioning in SDM networks. For the first time, constraints and performance of state-of-the-art MGDM devices are considered for a real implementation of the MGDM network. A very advanced FMF supporting 15 spatial modes [26] is taken into account. The available 15 spatial modes can be divided in 5 groups, so 5 spatial super-channels per wavelength are achieved. Thanks to MGDM, the independent routing of each group is envisioned. With respect to [22,23], the availability of such a number of mode groups allows to exploit the real capabilities of MGDM, considering the higher number of possible combinations of excited mode groups. Indeed, the recent commercial availability of mode MUX/DEMUXs, based on multi-plane light conversion (MPLC) [27] to multiplex and demultiplex in an all-optical passive way the modes, leads to new constraints (due to the handling of 15 supported spatial modes) associated to relevant impairments (IGXT introduced during the mode multiplexing/demultiplexing) not addressed by previous studies. After travelling along the same network path and after the mode DEMUX, the polarization-division multiplexed (PDM) modes, belonging to the same mode group, are separated thanks to coherent detection, with reduced DSP complexity with respect to the full-MIMO approach. Mode MUX/DEMUXes are employed in each node to perform all-optical passive switching/aggregation enabling mode group routing.

The paper is organized as follows: first of all, we describe in detail the actual 5-group MGDM system analyzed in the paper. Then, we present the design of specialized node architectures, managing the wavelength/spectrum and the mode switching in different ways. In particular we discuss their implementation, considering the specific case of the 15 spatial modes handling. The proposed architectures are analyzed in terms of required equipment (type and number of node sub-components).

A Quality of Transmission (QoT) model [28] is exploited to analyze the impact of the linear and nonlinear impairments. In this paper, contrary to the approach adopted in other papers studying the performance in MGDM-based systems, we also consider the IGXT between different groups [29]. In the MGDM systems, the IGXT is actually accumulated not only during the FMF propagation, but it is also introduced in all the crossed mode MUX/DEMUX, thus it cannot be considered negligible; in particular, for adjacent groups it constitutes a relevant limitation to the transmission reach. Several combinations of mode groups per wavelength with different modulation formats are processed through the developed QoT model, in order to analyze the benefits introduced by MGDM from a network-level perspective.

Finally, a provisioning strategy is proposed for MGDM and the performance is analyzed with dynamic network simulations. Results show that MGDM systems employing state-of-the-art components and devices permit to increase traffic throughput with respect to the full-MIMO approach, while reducing the complexity of MIMO receivers.

II. MGDM IN CASE OF A 15 SPATIAL MODES SYSTEM

The analysis of the MGDM capabilities is based on the exploitation of an advanced FMF [26], which will be deployed in the metro ring of L'Aquila city in the frame of the research project FIRST [30]. The fiber is fabricated by DRAKA – Prysmian Group using standard multimode processes, which allows for tight process tolerances, yielding low differential mode group delays (<155 ps/km) with low attenuations (<0.22 dB/km), large effective areas (≥ 95 μm^2) and low bend losses. This fiber supports 9-LP modes, corresponding to 15 spatial modes. It is not possible to organize the transmission in 9 groups, constituted by the degenerate modes only, as some modes present the same effective refractive indexes, according to the index profile. As reported in Fig. 1, we organize the 15 spatial modes in 5 groups, corresponding to 5 spatial super-channels: group a) includes the LP01 mode; group b) the degenerate LP11a and LP11b; group c) LP02, LP21a and LP21b; group d) LP12a, LP12b, LP31a, LP31b; and finally group e) LP03, LP22a, LP22b, LP41a, LP41b. A combination of mode groups, from the group a) in case of standard single-mode propagation up to 5 groups, can share the same light path.

The actual impact of the IGXT introduced during the mode multiplexing/demultiplexing is also analyzed starting from the performance of commercial devices. In fact, the mode MUX/DEMUX considered in our MGDM system is produced by CAI Labs (model PROTEUS-C-15) [31]. This MPLC-based device operates over the whole C band, handling the M=15 spatial modes. The IGXT introduced by the mode MUX/DEMUX is not negligible, but it impacts in a significant way on the system performance in terms of reach, also considering that the mode MUX/DEMUXs are present in each network node. The employment of this realistic device in our analysis allows to draw accurate conclusion on the feasibility of the MGDM system discussed in the paper.

At the transmitter side, it multiplexes up to 15 modes originating up to 5 groups. At the receiver side, after the mode demultiplexing, the modes belonging to the same group, multiplexed also in polarization by PDM, are coherently detected and processed all together by means of partial MIMO equalization. As reported in Fig. 2, with respect to the use of a

30x30 full MIMO requested to process all the 15 PDM spatial modes, the MGDM approach allows to reduce the MIMO complexity, employing at maximum a 10x10 MIMO to demultiplex the PDM modes inside the group e). The complexity of the MIMO DSP necessary to demultiplex the spatial modes inside each group could be further reduced by exploiting special FMFs, such as ring core fibers [32], limiting the number of spatial modes in each group.

Group	Spatial modes	
a)	LP01	
b)	LP11a, LP11b	
c)	LP02, LP21a, LP21b	
d)	LP12a, LP12b, LP31a, LP31b	
e)	LP03, LP22a, LP22b, LP41a, LP41b	

Fig. 1 Organization of the considered FMF spatial modes in 5 mode groups

III. ENABLING NODE ARCHITECTURES

This section introduces optical node architectures, designed for a ring topology (e.g., typically adopted in metro networks) exploiting the capabilities of MGDM, where MG switching is allowed. Accounting for MG switching represents a novelty with respect to other node architectures reported in literature, where strategies based on full MIMO are adopted. In these cases, mode switching at the intermediate nodes is prevented as all the modes are jointly routed from the source to the destination in order to perform a joint full MIMO at the receiver [3]. Or else all the modes must be always accessible at all network nodes along the path, to allow full MIMO, even if the modes would have different destinations [4]. The node architectures are presented and discussed also in view of a realistic implementation, employing state-of-the-art devices. The first architecture performs spectrum demultiplexing as initial step (Sec. IIIA), while the second presented architecture provides mode demultiplexing before spectrum switching (Sec. IIIB). Each architecture is shown focusing on the east-to-west direction; a symmetric solution is then assumed to handle west-to-east signals, providing a fully bidirectional architecture. The provided add&drop (A&D) modules then enable the selection of the proper direction, guaranteeing directionless capabilities. The actual implementation of the proposed node architectures employing state-of-the-art components and devices is also taken in account (Sec. IIIC). Finally, the node architectures are discussed in terms of necessary equipment (Sec. IIID).

A. MDM node with initial spectrum demultiplexing

Fig. 3 shows the node architecture based on spectrum demultiplexing as the initial step. The architecture presents an input and an output port, and A&D planes. At first, signals multiplexed in the spectrum and in space are demultiplexed in spectrum, separating the wavelengths by means of λ DEMUX operating in MDM condition (MDM λ DEMUX). Each wavelength channel carries mode groups that can be routed toward the output port or to the drop module to be received.

In case of the full MIMO approach, the spatial modes excited in the FMF per each wavelength, must be switched all together without any mode demultiplexing at the node level, in order to share the same path. The node assures flexibility in the spectral domain only. Figure 3a) illustrates a nodal degree (N=2) architecture based on a spatial switch (SW, e.g. MEMS) operating with multiple modes – repeated for all the wavelengths – which directs the signals toward the A&D or the passthrough (East port in the figure).
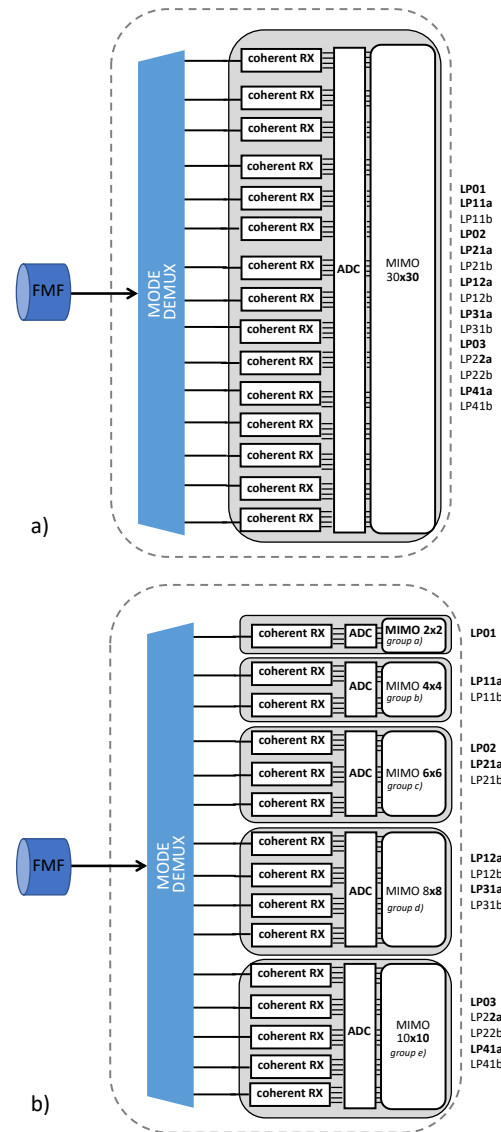
Fig. 2 MDM coherent detection in case of: a) full MIMO approach; b) MGDM approach.

On the contrary, to exploit also the spatial domain for networking, mode unbundling is necessary after the spectrum DEMUX by means of a mode DEMUX per each wavelength (Fig. 3b). Before entering the switch, modes are demultiplexed given that currently available switches can operate by switching a single mode or multiple modes, but toward the same output port, without the possibility to multiplex and

demultiplex the modes. In case of *M* spatial modes, mode unbundling requires *2Mx2M* SW. Of course, when MGDM approach is applied, the modes inside the same group, after the unbundling, must be switched in the same direction in the SW. Otherwise, the modes inside the same mode group must remain bundled by means of mode-group MUX/DEMUX and switched together toward the drop or the East port (Fig. 3c). The mode groups are then multiplexed together before entering the final wavelength MUX. *2Gx2G* SW is required in this case, able to manage the *G* groups. We assume colorless, directionless, and groupless (i.e., any group can be directed toward any port) A&D.

Fig. 4 shows the details of the A&D planes in case of the node architecture managing the *G* mode group described in Fig. 3c. For each wavelength, the added channels organized in *G* groups through mode MUXs can be addressed to the East or West port by means of the SW (Fig. 4a). On the other side, at the Drop plane, mode groups coming from the West or East port can be received after mode demultiplexing (Fig. 4b). A SW can be configured to direct the signals to the proper receiver.

B. MDM node with initial group demultiplexing

Fig. 5 shows the node architecture exploiting mode demultiplexing as the initial step and then spectrum switching. As in the previous case, the architecture is designed for a ring topology and includes the A&D functionalities. As shown in Fig. 5a, signals multiplexed in the spectrum and in mode groups are demultiplex by a mode DEMUX for mode unbundling. Then, each mode (carrying WDM signals) enters a wavelength selective switch (WSS), possibly supporting flexible grid, to be switched toward the output port or the drop plane. A proper configuration of the WSSs enables the switching of a given portion of spectrum in a specific mode. Thus, a given wavelength on a given mode may be directed to the output port or to the drop plane. When MGDM approach is applied, the modes inside the same group, must be directed in the same direction. Finally, before the output port a mode MUX multiplexes again all the modes before entering the FMF. Each WSS per group (Fig. 5b) accepts signals also from the add module. If WSSes operating in MDM condition are available (MDM WSSes), the modes inside the same mode group must remain bundled by means of mode-group MUX/DEMUX and routed together toward the drop or the output port, as shown in Fig. 5b. Figure 6 reports also the A&D plane for this configuration, managing the mode groups instead of the spatial modes. In particular, each WSS permits to direct an added signal toward East or West. At the drop side, the first set of WSSes permits to select signals from East or West; the spectrum DEMUX enables a receiver to detect mode demultiplexed signal at a specific frequency.
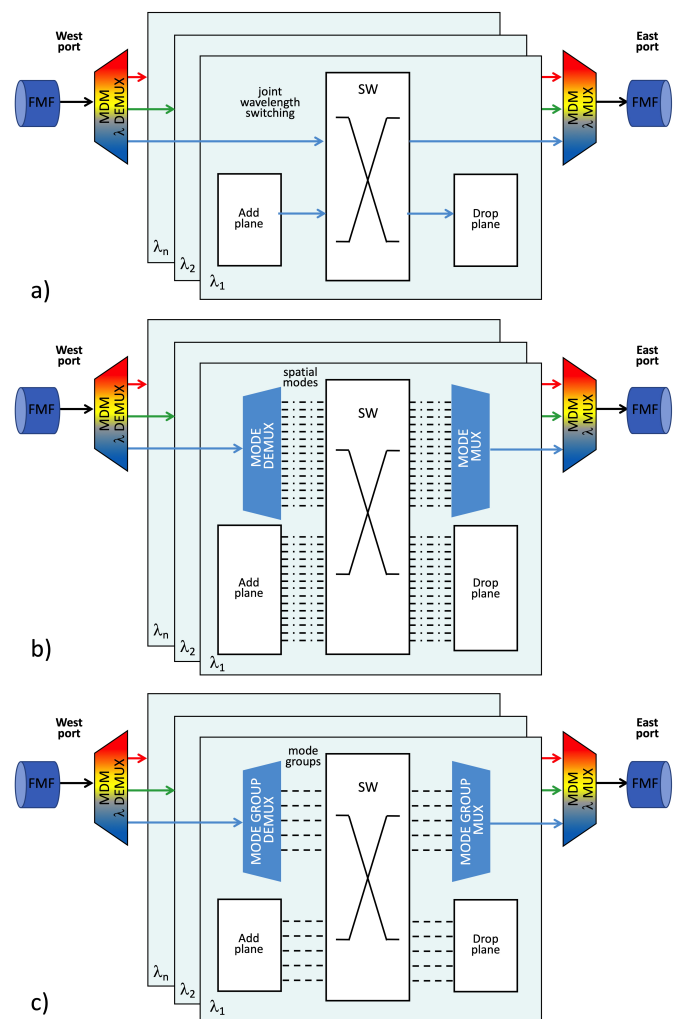

Fig. 3. MDM node architecture based on spectrum demultiplexing as initial step (SW with nodal degree *N*=2): a) without mode DEMUX for joint mode switching in case of full MIMO approach; b) with mode DEMUX and c) with mode group DEMUX.

C. Implementation of MDM nodes

Regarding the feasibility of node architectures characterized by spectrum demultiplexing as the initial step described in Fig. 3 and Fig. 4, SW can be realized by free-space switches (MEMS-based) and free-space beam-splitters, providing switching functionality, also with multiple modes [33]. Just the sizes of the MEMS mirrors and beam-splitters need to be increased to accommodate the multimode beams, but the SW design remains the same with respect to single-mode operation.

Moreover, MPLC-based devices considered in this paper [31] can be employed both for mode multiplexing/demultiplexing (in case of unbundling of all the spatial modes) and for mode group multiplexing/demultiplexing (in case of unbundling of the mode groups), even with a significant number of spatial modes M. However, the main issue in the practical realization of this kind of node architectures remains the MDM λ MUX/DEMUX [34]. Planar lightwave circuit (PLC) waveguides implementation is not realistic, while diffractive free-space schemes are available for low numbers of spatial modes *M*, but their scalability to higher mode numbers (e.g.
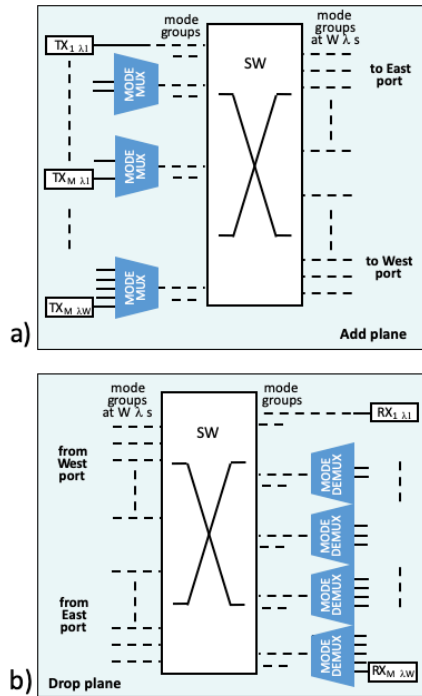
M=15) could be difficult.

Fig. 4. A&D planes for the MDM node architecture based on spectrum demultiplexing as initial step, with unbundled mode groups (Fig. 3c).

On the other side, for the implementation of a node architecture characterized by mode demultiplexing as the initial step reported in Fig. 5 and 6, MPLC-based devices can multiplex/demultiplex the spatial modes or the mode groups also with a significant number of spatial modes M, as described before. In particular, in this kind of node architecture, the operation of the considered mode MUX/DEMUX across the full band allows to manage the modes transporting the WDM channels. The main issue in this node architectures is the WSS. Current WSSes support just the fundamental mode only, hence the mode DEMUX must demultiplex all the spatial modes, as in case of Fig. 5a. In this case, M parallel single-mode WSSes are necessary. On the contrary, if the mode group DEMUX demultiplexes just the mode groups, as in Fig. 5b, a MDM WSS is necessary. Free-space design can be effectively exploited, but research in this direction is relatively scarce. MDM WSSes must handle many free-space beams (corresponding to the modes inside the same group) to switch them into the same output port.

This requested feature impacts on the optical design of the WSS in terms of spectral channel characteristics. Owing to the different clipping experimented by each mode beam at the steering plane, where the beams are spatially dispersed, mode-dependent passbands and spectrally dependent mode mixing at channel edges are achieved. This leads to a larger spectral transition bandwidth between the pass-band and the block-band, requiring larger guard bands between adjacent WDM channels in order to be switched without incurring spectral filtering and channel crosstalk [33, 35]. In [36] the authors provide design guidelines for MDM WSS supporting six spatial modes, which are easily extendable to higher mode
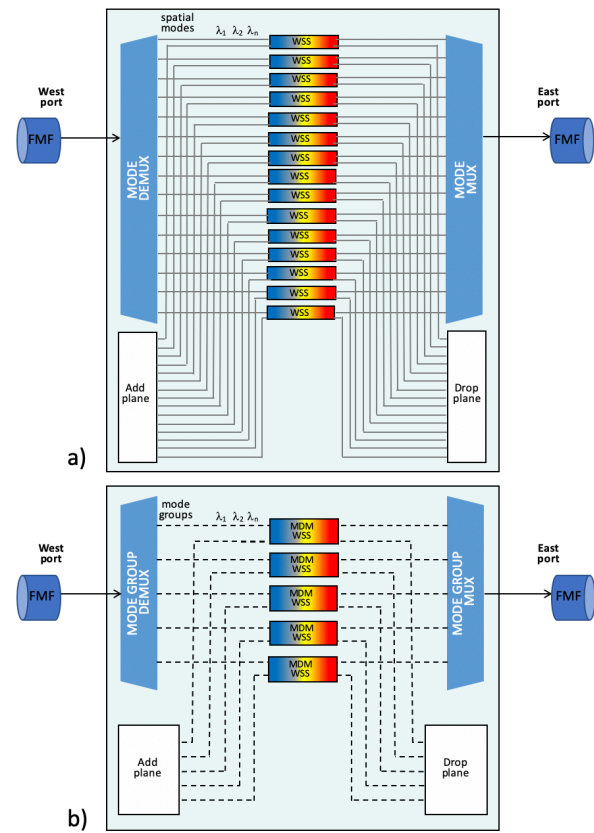

Fig. 5. MDM node architecture based on mode demultiplexing as initial step (SW with nodal degree N=2) with mode DEMUX and WSS (a) and mode group DEMUX and MDM WSS (b).
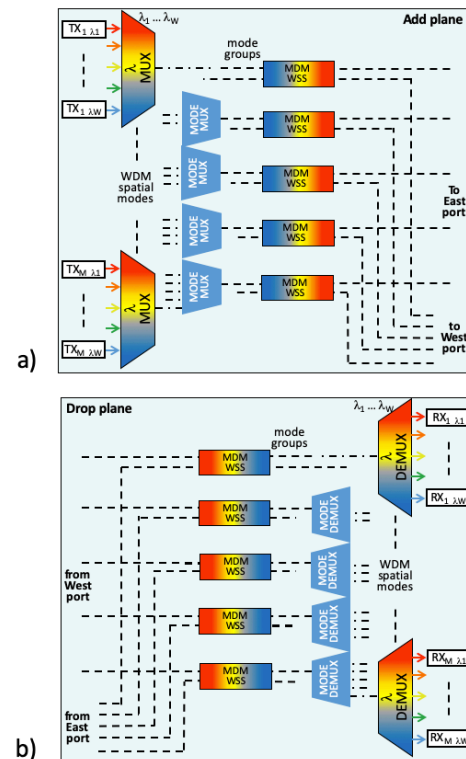

Fig. 6. A&D planes for the MDM node architecture based on mode demultiplexing as initial step with unbundled mode groups (Fig. 5b).

counts, using the Hermite-Gaussian beam approximation for the mode propagation. In the case of the FMF considered in this paper, supporting 5 mode groups, the maximum number of spatial modes inside a single group is 5 for the group e). Following the guidelines reported in [36], a MDM WSS handling 5 modes is therefore feasible.

D. MDM node architectures equipment discussion

Table I summarizes the components and sub-systems required to implement the MDM node architectures described in Sec. IIIA and IIIB. The analysis focuses on a single node since by scaling with the number of nodes it is immediate to derive the overall network requirements in terms of components and devices. M is the total number of spatial modes ($M=15$ for the implementation analyzed in this paper), G is the number of mode groups ($G=5$), and W is the number of WDM channels. The nodal degree N is 2.

The node architectures described in Sec. IIIA use ($2W+2$) spatial switches: $2W$ to handle both East and West directions for each wavelength plane, one switch at the add side, and one switch at the drop side.

In the case of joint mode switching corresponding to full MIMO (Fig. 3a), the $2W$ SWes are of dimension $2x2$. The two additional switches used in add (and drop) are of maximum dimension $2W$ x $2W$, enabling the selection of each optical flow toward any specific wavelength in each direction plane.

In the case of mode MUX/DEMUX (Fig. 3b), the 2W SWes are of dimension $2M$ x $2M$ (or alternatively a single SW of dimension $4WM$ x $4WM$) while the two additional SWes for the A&D plane are of dimension ($2WM$ x $2WM$). Note that among the WM switch ports on the client side up to T will be actually utilized.

In the case of the proposed architecture exploiting mode-group MUX/DEMUX (Fig. 3c), the $2W$ SWes are of dimension $2G$ x $2G$ (or alternatively a single SW of dimension $4WG$ x $4WG$). The two additional A&D plane SWes are of maximum dimension ($2WG$ x $2WG$). Thus, the unbundling of the modes belonging to the same mode group (Fig. 3c) allows to reduce the dimension of all the SWes (both in the node and in the A&D plane).

In terms of the number of mode MUX/DEMUX, none are needed in the node architecture of Fig 3a based on full MIMO, while $4W$ are required in case of Fig. 3b and Fig. 3c, considering both directions.

The add/drop module for full MIMO (Fig. 3a) requires $2W$ mode MUX/DEMUX, none are needed in the architecture of Fig. 3b, and $2W(G-1)$ are required in the case of Fig. 3c. In this last case of mode grouping, they are necessary to multiplex/demultiplex the modes inside the groups at the A&D plane (the group a) constituted just by one mode does not require mode multiplexing/demultiplexing). The number of mode MUX/DEMUX is higher than the previous cases, however, their implementation is of limited complexity since they operate with a low number of ports. In case of the 15-mode FMF considered in the paper, for the highest group e) just 5 spatial modes must be multiplexed/demultiplexed. Hence, the mode MUX/DEMUX implements at maximum as $1x5$ instead of $1x15$.

TABLE I
MDM NODE EQUIPMENT REQUIRED (NODAL DEGREE N = 2)

	MDM node based on λ demux as initial step with mode DEMUX (Fig. 3b)	MDM node based on λ demux as initial step with mode group DEMUX (Fig. 3c)	MDM node based on mode demux as initial step with mode group DEMUX (Fig. 5a)	MDM node based on mode demux as initial step with mode group DEMUX (Fig. 5b)
λ MUX/ DEMUX	-	-	2M of 1xW	2G of 1xW
MDM λ MUX/ DEMUX	4 of 1xW	4 of 1xW	-	-
mode or group MUX/ DEMUX	4W of 1xM	4W of 1xG + 4W(G-1) with dimension depending by the number of modes in each group	4 of 1xM	4 of 1xG + 4(G-1) with dimension depending by the number of modes in each group
Spatial SW	2W of (2Mx2M) + 2 of (2WM x 2WM)	2W of (2Gx2G) + 2 of (2WG x 2WG)	-	-
Single Mode WSS	-	-	2M of 2x2 + 2M of 2x2	-
MDM WSS	-	-		2G of 1x2 + 2G of 2x2

Note that the architectures in Sec. IIIA exploit 2 MDM spectrum MUX/DEMUX, difficult to be implemented, as highlighted in the previous paragraph.

The node architectures described in Sec. IIIB based on spectrum demultiplexing as initial step are here discussed.
In the case of the architecture where all modes can be treated independently (Fig. 5a), four mode MUX/DEMUX of dimension 1xM are needed in the pass-through considering both directions. Also, in the case of the architecture of Fig. 5b, the number of mode-group MUX/DEMUX is four. Managing with the groups, they can be implemented of dimension 1xG, instead of 1xM.

The availability of MDM WSSes discussed in Sec. IIIC reduces the number of the required WSSes, from M to G in this latter architecture. The dimension of the WSS to achieve a fully non-blocking solution is $2x2$ in both cases of Fig. 5a and Fig. 5b.

The A&D module related to Fig. 5a requires a number M of λ MUX/DEMUX of dimension up to $Wx1$ followed by M WSSes of dimension $2x2$ to handle both directions. No mode MUX/DEMUX are required in this architecture.

The A&D module related to Fig. 5b requires a number M of λ MUX/DEMUX of dimension up to $Wx1$ followed by G MDM WSSes of dimension $2x2$ to handle both directions. In addition, both the add and the drop requires ($G-1$) mode MUX/DEMUX of dimension depending by the number of modes in each group. For the MGDM system with M=15 considered in this paper, the node architecture in Fig. 5b based

on group unbundling requires 4 1x5 mode-group MUX/DEMUX, 8 mode MUX/DEMUX managing at maximum 5 modes, and 20 MDM WSSes.

As summarized in Tab. I, the complexity of the architectures in Fig. 3 is dominated by the number of mode/group MUX/DEMUX and SWes which are proportional to the number of wavelengths. Instead, the number of mode/group MUX/DEMUX and WSSes in Fig. 5 depends on the number of modes or groups. Regarding λ MUX/DEMUX, only four of the MDM type are needed in the architectures of Fig. 3, while 2M or 2G of standard λ MUX/DEMUX are required in Fig. 5a and 5b, respectively. Moreover, by comparing the architectures of Fig. 5a and 5b, the possibility to operate on mode groups in the multiplexing/demultiplexing operation instead on the single spatial mode reduces the number of devices. Indeed, even if the architecture of Fig. 5b requires 2(G-1) additional mode MUX/DEMUX, the overall number of

the other components is reduced with respect to Fig. 5a (WSSs are reduced from 4M to 4G and λ MUX/DEMUX from 2M to 2G).

IV. MGDM-BASED QoT ESTIMATOR

To avoid great computational complexity [37,38], a suitable simulation tool [28] based on the so-called Gaussian noise model [39,40] has been developed for evaluating the QoT.. In addition to the erbium doped fiber amplifier (EDFA) amplified spontaneous emission (ASE) and the signal distortion due to the Kerr nonlinear effects in the WDM fiber propagation, in this paper we take into account also the in-band IGXT, introduced as an additional source of Gaussian noise. In the estimator we consider the IGXT accumulated during the 15-mode FMF

TABLE II
MODE MUX/DEMUX PERFORMANCE ASSESSMENT: IGXT MEASURED IN THE EXPERIMENTAL SETUP CONSTITUTED BY A PAIR OF MUXs/DEMUXs IN BACK-TO-BACK.

Unit[dB]	LP01	LP11a	LP11b	LP02	LP21a	LP21b	LP31a	LP12a	LP12b	LP31b	LP03	LP41a	LP22a	LP22b	LP41b
LP01	NA	-19.9	-19.9	-28.9	-28.9	-28.9	-28.8	-28.8	-28.8	-28.8	-34.2	-34.2	-34.2	-34.2	-34.2
LP11a	-22.7	NA	NA	-21.7	-21.7	-21.7	-27.1	-27.1	-27.1	-27.1	-27.9	-27.9	-27.9	-27.9	-27.9
LP11b	-20.5	NA	NA	-21.0	-21.0	-21.0	-25.4	-25.4	-25.4	-25.4	-28.8	-28.8	-28.8	-28.8	-28.8
LP02	-28.0	-21.6	-21.6	NA	NA	NA	-23.2	-23.2	-23.2	-23.2	-26.5	-26.5	-26.5	-26.5	-26.5
LP21a	-31.3	-22.6	-22.6	NA	NA	NA	-21.4	-21.4	-21.4	-21.4	-27.5	-27.5	-27.5	-27.5	-27.5
LP21b	-27.8	-23.4	-23.4	NA	NA	NA	-21.9	-21.9	-21.9	-21.9	-25.1	-25.1	-25.1	-25.1	-25.1
LP31a	-27.9	-28.3	-28.3	-21.4	-21.4	-21.4	NA	NA	NA	NA	-18.6	-18.6	-18.6	-18.6	-18.6
LP12a	-31.6	-26.1	-26.1	-22.6	-22.6	-22.6	NA	NA	NA	NA	-20.6	-20.6	-20.6	-20.6	-20.6
LP12b	-32.2	-25.3	-25.3	-24.8	-24.8	-24.8	NA	NA	NA	NA	-20.3	-20.3	-20.3	-20.3	-20.3
LP31b	-27.1	-24.1	-24.1	-21.6	-21.6	-21.6	NA	NA	NA	NA	-18.5	-18.5	-18.5	-18.5	-18.5
LP03	-35.9	-29.3	-29.3	-21.3	-21.3	-21.3	-20.5	-20.5	-20.5	-20.5	NA	NA	NA	NA	NA
LP41a	-30.4	-23.9	-23.9	-23.5	-23.5	-23.5	-18.0	-18.0	-18.0	-18.0	NA	NA	NA	NA	NA
LP22a	-38.1	-28.3	-28.3	-26.7	-26.7	-26.7	-20.4	-20.4	-20.4	-20.4	NA	NA	NA	NA	NA
LP22b	-35.1	-27.8	-27.8	-22.6	-22.6	-22.6	-18.6	-18.6	-18.6	-18.6	NA	NA	NA	NA	NA
LP41b	-29.3	-24.1	-24.1	-23.9	-23.9	-23.9	-18.3	-18.3	-18.3	-18.3	NA	NA	NA	NA	NA

propagation and induced by the coupling of the MPLC MUXs/DEMUXs. The considered FMF presents a weak coupling between modes of different groups and the IGXT due to FMF propagation used in our simulation is -25 dB/km between the nearest neighbor mode groups [41], while for the mode MUX/DEMUX crosstalk we exploit the data measured on the employed MPLC-based PROTEUS-C-15. Table II reports the MUX/DEMUX performance assessment, with IGXT averaged over the C band measured in an experimental setup constituted by a pair of MUX/DEMUX in back-to-back and an ASE source. By measuring the input power and the power at each output, we retrieve the coupling efficiency and the IMXT for all the modes. In order to neglect the effect of intra-mode group mixing inside the fiber in the calculation of the IGXT, the cross-talk is averaged for each input over the modes of the same mode group [31]. Our experimental measures confirm that in actual MGDM systems the IGXT cannot be neglected, in particular for adjacent groups, contrary to [29]. At first, in the simulations, we have optimized the launch power in case of WDM propagation considering the intra-modal nonlinear (NL) effects and assuming for all the

modes the same nonlinear coefficient of the fundamental LP_{01} mode. We obtained a power of 0 dBm; this is a worst case for intra-modal NL effects, since the NL coefficient of the fundamental mode is expected to be the highest one [39]. The inter-modal NL effects have been evaluated for the worst combination of MGs and propagation distances, resulting negligible with respect to the linear crosstalk contributions [39]. In the following complete analysis then, just intra-modal NLs and linear contributions have been accounted for, as in the considered network the reach is mainly limited by the IGXT.

Moreover, we consider propagation over amplified multi-span links with one EDFA for each span, exactly compensating for the span losses. The losses due to the crossing of a node are completely compensated by a further EDFA: hence, the node model includes the introduction of ASE such as in case of span propagation.

In particular, we take into account 28-Gbaud symbol rate and 37.5 GHz WDM channel spacing, EDFA noise figure (NF) of 6 dB, fiber attenuation of 0.22 dB/km and chromatic dispersion of 16.7 ps/(nm km). 106 WDM channels are simulated to evaluate the non-linear effect impairments. The degradation in terms of the error-vector

magnitude (EVM) at 28-Gbaud is evaluated for PDM-QPSK and PDM-16QAM modulation formats, for the different combinations of considered mode groups. Finally, the maximum transmission reach L (corresponding to the maximum number of span hops H) is analytically calculated, in a closed form, from the EVM assuring the target BER of $4 \cdot 10^{-3}$ (suitable for the exploitation of 7-% hard decision FEC). The results are reported in Table II, not considering any impairment due to the mode-dependent loss (MDL). We have actually verified by simulations that the impact of MDL is limited in the considered metro ring scenario, being MDL less than 0.02 dB/km for propagation in the 9-LP FMF [26] and less than 2 dB for the mode MUX/DEMUX crossing (from measurements). The detrimental effect of the reduction of the OSNR in the modes with higher losses is not so relevant in presence of significant IGXT, leading to a reduction of the reach not greater than a span length in all simulated cases. The impact of MDL could be not negligible if the employment of devices such as the ones described in Section III enabling the MGDM-based node architectures (i.e. the MDM WDM MUX/DEMUX and the MDM WSS) introduces significant MDL.

The QoT estimation allows to identify the supported whole capacity (equivalent bit rate value R) and the maximum length L, achieved as described before, depending on the adopted modulation format and mode group combination, where S is the total number of spatial modes. We introduce also the parameter C indicating the DSP complexity of the receiver (expressed as the number of equalizers [42] employed in the receiver DSP normalized to ones adopted in case of 2x2 MIMO for standard single mode detection). The complexity evaluation is based on the MGDM receiver scheme reported in Fig. 2b, exploiting the all-optical mode DEMUX and compliant with standard coherent RX employed for PDM single-mode detection (C=1 corresponding to 2x2=4 equalizers). By way of example, the combination of mode groups a)+c) requires at the receiver a 2x2 MIMO for the mode LP01 and a 6x6 MIMO to demultiplex the three PDM modes in group c). This means a total amount of equalizers equal to 4+36=40, corresponding to a normalized DSP complexity C=10.
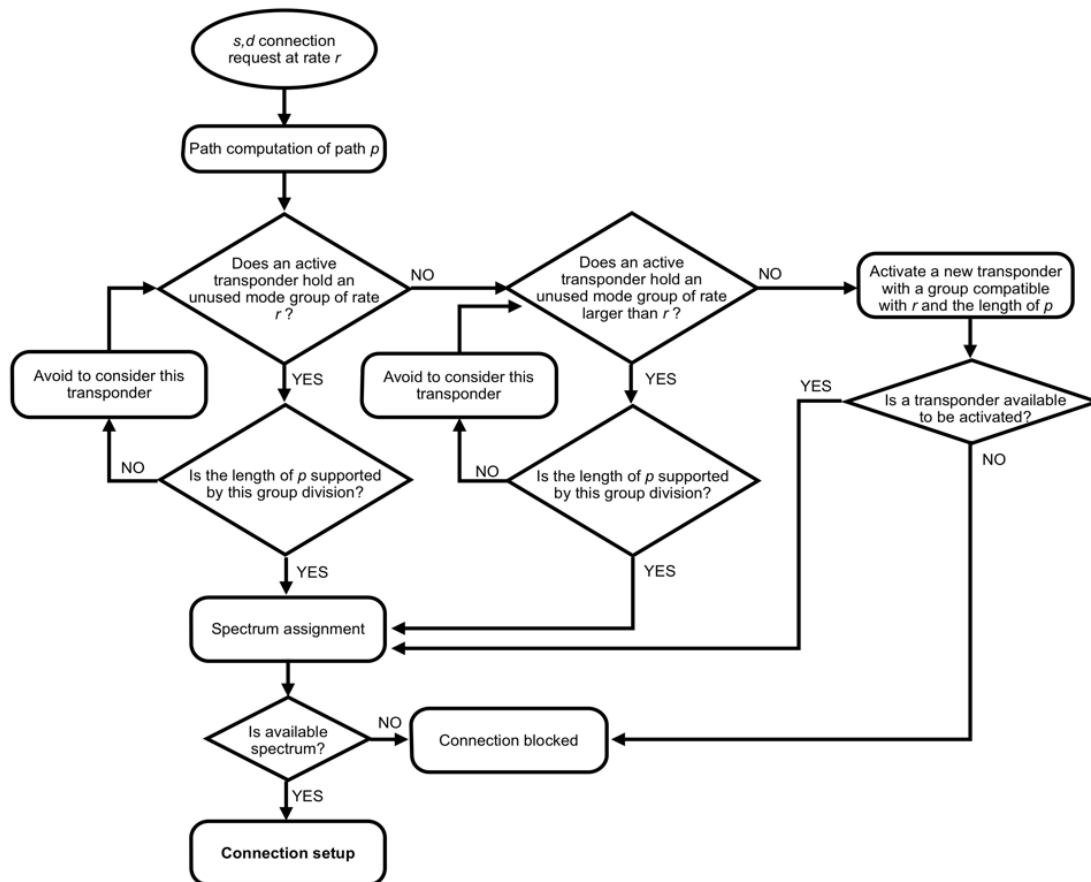

Fig. 7 Flow chart of the provisioning

As discussed before, the proposed scheme allows to reduce the MIMO complexity with respect to the full MIMO approach (C=225).

Two ring networks with spans of 25 km or 50 km are respectively considered in our simulations. Such a network may correspond to rings covering suburban areas as considered in [40] for 5G applications. For this network, the optimal transmitted power per single wavelength and per single spatial mode (with two polarizations) is 0 dBm. The performance results for 25-km and 50-km span lengths are shown in Table III. MGDM approach enables transponders supporting multiple optical flows, similarly to a sliceable transponder [44,45]. As an example, by exploiting PDM-QPSK format, the a+c+e group combination (corresponding to

9 spatial modes) supports three independent optical flows with rates of 100, 300, and 500 Gb/s, respectively, with the maximum reach L limited to 100 km (in the case of 25 km spans) by the IGXT accumulated during the FMF propagation and introduced by the mode MUXs/DEMUXs. In this case, the DSP complexity factor C is 35. Each of the three optical flows can serve an optical connection and can be routed along the network independently of the other two, crossing up to 4 nodes.

V. PROVISIONING BASED ON MGDM

The flow chart of the proposed MGDM-based provisioning is presented in Fig. 7. Assuming a connection request of rate r between a source-destination pair s-d, a path p is first computed (e.g., shortest path). Then, a transponder is selected. Preference is given to the already active transponders since each new activation increases costs (or complexity) associated to the transponders.

TABLE III
SUPPORTED REACH, BIT RATE AND COMPLEXITY PER MODE GROUP COMBINATION WITH 25KM AND 50KM SPANS

Mode groups	S	C	R [Gb/s]	L [km]		H	
				25km spans	50km spans	25km spans	50km spans
PDM-QPSK							
a	1	1	100	1425	4250	57	85
a + c	4	10	100+300	250	350	10	7
a + d	5	17	100+400	650	1150	26	23
a + c + e	9	35	100+300+500	75	100	3	2
a+b+c +d+e FULL MIMO	15	225	1500	1675	5350	67	107
PDM-16QAM							
a	1	1	200	300	900	12	18
a + c	4	10	200+600	50	50	2	1
a + d	5	17	200+800	100	250	4	5
a+b+c +d+e FULL MIMO	15	225	3000	350	1150	14	23

Among the already active transponders, preference is given to the ones with available groups of modes supporting exactly the requested rate, with the aim of avoiding an under usage of optical flows capacity. Thus, an active transponder is first searched at both s and d, with an available group of modes supporting a rate equal to r and the length of p. If these conditions are not met, an active transponder is searched at both s and d, with an available group of modes supporting a rate larger than r and supporting the length of p. If also these conditions are not met, a new transponder is activated with a group combination compatible with the requested rate r and the length of p. After transponder selection, spectrum assignment is performed considering in our study signals switched in 37.5 GHz. We introduce the *wavelength-group*

first fit assignment by building up from the traditional first-fit spectrum assignment.
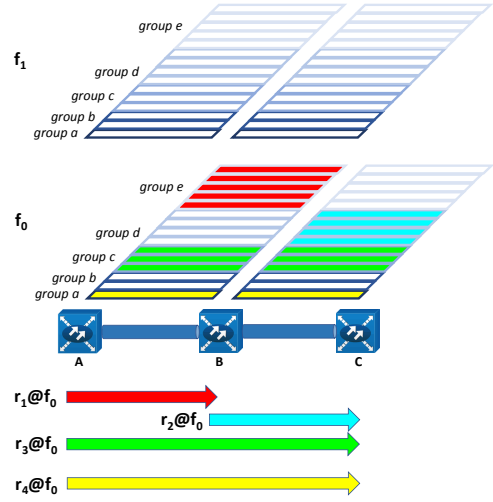

Fig. 8 Wavelength-group first-fit assignment strategy

To describe the considered wavelength-group first-fit assignment strategy, a portion of a network consisting of two links is assumed (see Fig. 8). The following four connections (r_i) are already established in this network, all satisfying the length/rate requirements of Table III using PM-QPSK. Connection r_1 of 500Gb/s on f_0 and group e in the link AB; r_2 of 400Gb/s on f_0 and group d in the link BC; r_3 of 300Gb/s on f_0 and group c in the links AB and BC; r_4 on f_0 and group a in AB and BC. Different connections may share the same portion of spectrum. As an example, on the link AB, r_1, r_3, and r_4 share the same portion of spectrum at f_0, given that they use different groups. Then, a new request r_5 arrives from A to C of 200 Gb/s: such rate can be successfully accommodated on group b at f_0 along that links. On the contrary, if the r_5 request was at 500 Gb/s, such a rate is satisfied by group e. However, such group is used at f_0 on that links and the lowest-indexed frequency offering group e in the link BC is f_1. Thus, the assignment strategy first identifies the suitable group. Afterwards, the lowest indexed wavelength offering the selected group in all the links of the computed path is selected. Guard bands are not assumed in this manuscript, however XPM and inter-modal crosstalk are considered in the QoT estimation.

Then, the connection is set up. A connection request is blocked when no transponder can be selected or when no available spectrum (satisfying the continuity constraint) is present along p.

VI. PERFORMANCE EVALUATION

Dynamic network simulations are carried out on a custom-built C++ simulator to compare a MGDM-based network a full-MIMO-based network. A ring topology of 12 nodes and 25-km or 50-km links is assumed, as previously stated, and also a Spanish mesh network of 31 nodes and 56 links of 50-km length. Traffic follows a Poisson process with mean inter-arrival time $1/\lambda$. Connection holding time is exponentially distributed with average $1/\mu$=500s. Traffic load, expressed as λ/μ, is varied through λ. The requested bit rate is randomly

selected among the following values: 100, 200, 300, 400, 500, 600, 800, 1500, 3000 Gb/s, reflecting the rate values in TABLE III.

In the full-MIMO-based network, each bit rate is supported by a single (a+b+c+d+e)-full-MIMO transponder. Path computation is shortest path and wavelength assignment first fit. Nodes are equipped with 30 transponders. The approaches are compared in terms of overall blocking probability; blocking probability contributions; average transponder complexity per node.

Fig. 9 shows the overall blocking probability as a function of traffic load in the ring with 25-km links. The lowest blocking probability is obtained by the proposed MGDM approach, which offers more flexibility: each transponder can serve more connections, each one occupying 37.5 GHz. Thus, MGDM uses a lower number of transponders than full MIMO. This result is also supported by Fig. 10, which shows the blocking probability contributions (i.e. blocking due to the lack of transponders and of spectrum satisfying the continuity constraint). Single mode architecture experiences high blocking probability both due to transponders and spectrum. With MGDM and full-MIMO, the blocking is mainly dominated by transponders, which are more efficiently used by MGDM. As an example, with full MIMO and MGDM, 28% and 6% of transponder resources, respectively, are used at 100 Erlang, while 55% and 11% at 200 Erlang. Spectrum blocking of MGDM is larger than the one of full MIMO because with the former more connections are accommodated in the network, thus consuming more spectrum.
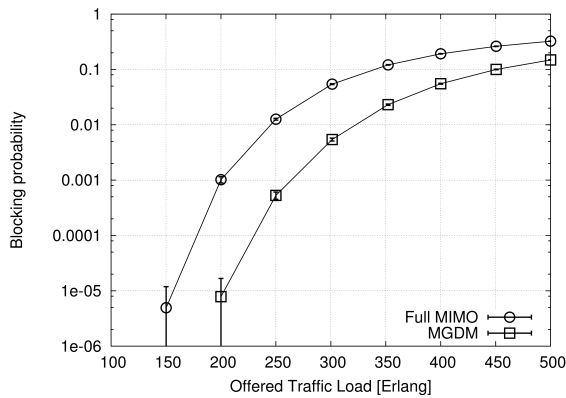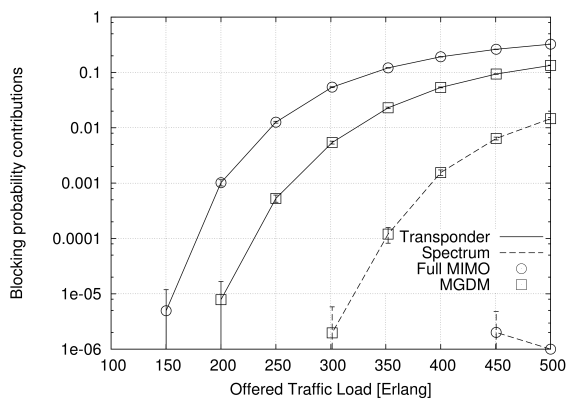
Fig. 10 Blocking probability contributions in the ring with 25-km links
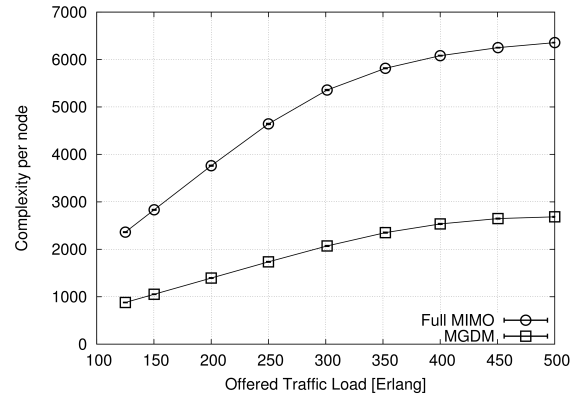

Fig. 11 Complexity per node vs. traffic load in the ring with 25-km links

Fig. 11 shows the average complexity per node versus traffic load in the ring with 25-km links: MGDM permits to strongly reduce the complexity per node with respect to full MIMO.

Finally, Fig. 12 shows the overall blocking probability as a function of traffic load in the ring with 50-km links. The behavior of the ~~three~~ two methods is confirmed and MGDM achieves the lowest blocking probability. Comparing Fig. 9 with Fig. 12, – the rings with 25-km and 50-km links, respectively –full MIMO approach presents the same performance. This is due to the fact that, as shown in Tab. III, its optical reach (L) is larger than the ring. MGDM better performs with span of 25 km. Indeed, as shown in Tab. III, especially for critical group combinations (i.e., whose optical reach L is shorter than the longest shortest path in the ring), with 25 km, more hops H are acceptable with respect to with 50 km (e.g., as it happens for a+c+e and a+c); thus, more source-destination pairs can be covered with that group combinations.

Fig. 9 Blocking probability as a function of traffic load in the ring with 25-km links
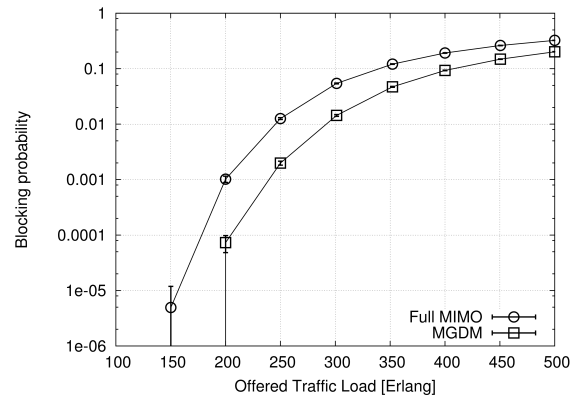

Fig. 12 Blocking probability as a function of traffic load in the ring with 50-km links
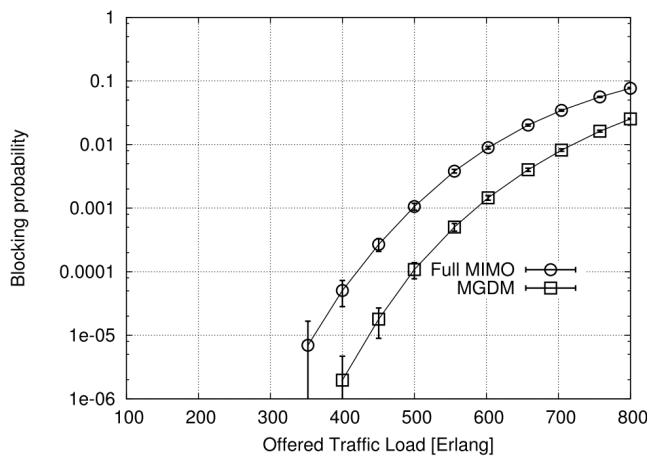
Fig. 13 Blocking probability as a function of traffic load in the mesh topology

Finally, Fig. 13 presents the blocking probability vs. traffic load in the mesh network. Also in this case, results confirm that MGDM provides a lower blocking compared to the more complex full MIMO. In particular, blocking probability is reduced of around one order of magnitude by MGDM at loads corresponding to realistic network utilizations (i.e., blocking probability below 0.01).

VII. CONCLUSION

We consider MGDM in SDM optical networks by taking into account a FMF supporting up to 5 mode groups: the availability of such a number of mode groups allows to exploit different combinations of mode groups excited in the fiber with the aim to minimize the IGXT. This opportunity offered by the considered FMF has a strong impact on the network provisioning analysis, allowing to better evaluate the real capabilities of MGDM. Node architectures, designed for a ring topology, exploiting MGDM to reduce the MIMO complexity at the receiver side and to allow the mode groups to have different destinations in the network are proposed, with respect to node schemes where all the modes are jointly routed in order to perform joint full MIMO. Two nodes architecture supporting color-less and direction-less add&drop and passthrough were presented: i) the first architecture demultiplexes the spectrum then switches modes (or groups); ii) the second architecture first demultiplexes the modes (or groups) then switches the spectrum channels. A discussion of the state-of-the art on the components enabling the presented node architecture was provided together with a scalability analysis at varying the number of channels, modes, and groups. Then, a QoT model was presented accounting for realistic IGXT obtained also by commercial mode MUX/DEMUX characterization, showing that IGXT cannot be neglected in the MGDM analysis, contrary to the approach adopted in other papers studying the performance in MGDM-based systems. Such model is essential for connection provisioning in order to assess the QoT of optical connections, which are identified by a portion of spectrum and a group of modes traversing a set of nodes and links. A connection provisioning scheme accounting for QoT in an MGDM network was proposed with the aim of limiting the number of used transponders. Simulations were carried out comparing the proposed approach with a full-MIMO SDM network. Simulations have shown that MGDM achieves higher throughput increase while limiting the complexity of MIMO receivers with different link span lengths. Future studies will investigate MGDM over parallel fibers, e.g. in terms of node architectures, migration/upgrade scenarios (e.g., pay-as-you-grow, brown/green deployment).

REFERENCES

[1] K. Kitayama, N.P. Diamantopoulos, "Few-Mode Optical Fibers: original motivation and recent progress," *IEEE Communications Magazine*, 163-169 (2017).

[2] R. Ryf et al., "Mode-Division Multiplexing over 96 km of Few-Mode Fiber using coherent 6x6 MIMO processing," Journal of Lightwave Technology, vol. 30, 4, 521 (2012).

[3] R. Muñoz, N. Yoshikane, R. Vilalta, et al., "Adaptive software-defined networking control of space division multiplexing super-channels exploiting the spatial-mode dimension," *Journal of Optical Communications and Networking,* vol. 12, no. 1, pp. A58-A69, 2020.

[4] F. Arpanaei, N. Ardalani, H. Beyranvand, S.A. Alavian, "Three-dimensional resource allocation in space division multiplexing elastic optical networks," *Journal of Optical Communications and Networking* 10 (12), 959-974 (2018).

[5] J. Perelló, J. M. Gené, A. Pagès, J. A. Lazaro and S. Spadaro, "Flex-grid/SDM backbone network design with inter-core XT-limited transmission reach," in *IEEE/OSA Journal of Optical Communications and Networking*, vol. 8, no. 8, pp. 540-552, Aug. 2016.

[6] C. Rottondi, P. Martelli, P. Boffi, L. Barletta and M. Tornatore, "Crosstalk-Aware Core and Spectrum Assignment in a Multicore Optical Link With Flexible Grid," in *IEEE Transactions on Communications*, vol. 67, no. 3, pp. 2144-2156, March 2019.

[7] Y. Li *et al.*, "Hardware programmable SDM/WDM ROADM," *2017 Optical Fiber Communications Conference and Exhibition (OFC)*, 2017.

[8] S. Fujii, Y. Hirota, H. Tode and T. Watanabe, "On-demand routing and spectrum allocation for energy-efficient AoD nodes in SDM-EONs," in *IEEE/OSA Journal of Optical Communications and Networking*, vol. 9, no. 11, pp. 960-973, Nov. 2017.

[9] H. Tode and Y. Hirota, "Routing, Spectrum, and core and/or mode assignment on space-division multiplexing optical networks [invited]," in *IEEE/OSA Journal of Optical Communications and Networking*, vol. 9, no. 1, pp. A99-A113, Jan. 2017.

[10] Q. Zhu *et al.*, "Service-Classified Routing, Core, and Spectrum Assignment in Spatial Division Multiplexing Elastic Optical Networks With Multicore Fiber," *2018 Asia Communications and Photonics Conference (ACP)*, 2018.

[11] M. Yaghubi-Namaad, A. G. Rahbar and B. Alizadeh, "Adaptive modulation and flexible resource allocation in space-division-multiplexed elastic optical networks," in *IEEE/OSA Journal of Optical Communications and Networking*, vol. 10, no. 3, pp. 240-251, March 2018.

[12] M. Yang, Y. Zhang and Q. Wu, "Routing, spectrum, and core assignment in SDM-EONS with MCF: node-arc ILP/MILP methods and an efficient XT-aware heuristic algorithm," in *IEEE/OSA Journal of Optical Communications and Networking*, vol. 10, no. 3, pp. 195-208, March 2018.

[13] G. Savva, G. Ellinas, B. Shariati and I. Tomkos, "Physical Layer-Aware Routing, Spectrum, and Core Allocation in Spectrally-Spatially Flexible Optical Networks with Multicore Fibers," *2018 IEEE International Conference on Communications (ICC)*, 2018.

[14] E. E. Moghaddam, H. Beyranvand and J. A. Salehi, "Crosstalk-Aware Resource Allocation in Survivable Space-Division-Multiplexed Elastic Optical Networks Supporting Hybrid Dedicated and Shared Path Protection," in *Journal of Lightwave Technology*, vol. 38, no. 6, pp. 1095-1102, 15 March15, 2020.

[15] J. M. Rivas-Moscoso, B. Shariati, D. M. Marom, D. Klonidis and I. Tomkos, "Comparison of CD(C) ROADM architectures for space division multiplexed networks," *2017 Optical Fiber Communications Conference and Exhibition (OFC)*, Los Angeles, CA, 2017, pp. 1-3.

[16] D. M. Marom *et al.*, "Survey of photonic switching architectures and technologies in support of spatially and spectrally flexible optical networking [invited]," in *IEEE/OSA Journal of Optical Communications and Networking*, vol. 9, no. 1, pp. 1-26, Jan. 2017

[17] M. Jinno, "Spatial Channel Cross-Connect Architectures for Spatial Channel Networks," in *IEEE Journal of Selected Topics in Quantum Electronics*, vol. 26, no. 4, pp. 1-16, July-Aug. 2020

[18] M. Jinno and T. Kodama, "Spatial Channel Network (SCN): Introducing Spatial Bypass toward the SDM Era," *2020 Optical Fiber Communications Conference and Exhibition (OFC)*, San Diego, CA, USA, 2020, pp. 1-3.

[19] J. M. Rivas-Moscoso, B. Shariati, A. Mastropaolo, D. Klonidis and I. Tomkos, "Cost Benefit Quantification of SDM Network Implementations based on Spatially Integrated Network Elements," ECOC 2016; 42nd European Conference on Optical Communication, 2016, pp. 1-3.

[20] R. Dar et al., "Cost-Optimized Submarine Cables Using Massive Spatial Parallelism," in Journal of Lightwave Technology, vol. 36, no. 18, pp. 3855-3865, 15 Sept.15, 2018, doi: 10.1109/JLT.2018.2841810.

[21] Peter J. Winzer, "Scaling Optical Fiber Networks: Challenges and Solutions," Optics & Photonics News 26(3), 28-35 (2015)

[22] C.E.M. Rottondi, P. Boffi, P. Martelli, M. Tornatore, "Routing, modulation format, baud rate and spectrum allocation in Optical metro rings with flexible grid and few-mode transmission," *IEEE Journal of Lightwave Technology* 35 (1), 61-70 (2017).

[23] C.E.M. Rottondi, P. Martelli, P. Boffi, M. Tornatore, "Transceivers and Spectrum Usage Minimization in Few-Mode Optical Networks," *IEEE Journal of Lightwave Technology* 37 (16), 4030-4040 (2019).

[24] N. Sambo, P. Martelli, P. Parolari, A. Gatto, P. Castoldi, P. Boffi, "Mode-group division multiplexing for provisioning in SDM networks", Proc. of ECOC 2020.

[25] https://www.cailabs.com/en/products/proteus

[26] P. Sillard, D. Molin, M. Bigot-Astruc, L. De Jongh, F. Achten, A.M. Velzquez-Benitez, R. Amezcua-Correa, C.M. Okonkwo "Low-Differential-Mode-Group-Delay 9-LP-Mode Fiber," *IEEE Journal of Lightwave Technology* 34,2, 425-430 (2016).

[27] G. Labroille, B. Denolle, P. Jian, P. Genevaux, N. Treps, J.F. Morizur, "Efficient and mode selective spatial mode multiplexer based on multi-plane light conversion," *Optics Express*, 22, 13, 15599-15607 (2014).

[28] P. Martelli and P. Boffi, "Crosstalk-Induced Penalty in Coherent Space-Division Multiplexing Transmission," *Proc. 2018 20th International Conference on Transparent Optical Networks (ICTON*), Bucharest (2018)

[29] R. Rumipamba-Zambrano, R. Munoz, R. Casellas, J. Perellò, S. Spadaro, A.E. Elfiqi, "Design and Assessment of FM-MCFs-Suited SDM-ROADMs with versatile Spatial Group Configurations and Unified QoT Estimator," *Journal of Lighwave Technology*, 38, 22, 6137-6152 (2020).

[30] http://prin2017first.univaq.it/news/

[31] N. Barré, B. Denolle, P. Jian, J.F. Morizur, G. Labroille, "Broadband, Mode-Selective 15-Mode Multiplexer based on Multi-Plane Light Conversion," *2017 Optical Fiber Communications Conference and Exhibition (OFC)*, Th2A.7, 2017.

[32] J. Liu, G. Zhu, J. Zhang, Y. Wen, X. Wu, Y. Zhang, Y. Chen, X. Cai, Z. Li, Z. Hu, J. Zhu, "Mode Division Multiplexing based on Ring Core Optical Fibers," *IEEE Journal of Quantum Electronics*, 54, 5, 0700118 (2018).

[33] D.M. Marom, P.D. Colbourne, A D'Errico, M.K. Fontaine, Y. Ikuma, R. Proietti, L. Zong, J.M. Rivas-Moscoso, I. Thomkos, "Survey of Photonic Switching Architectures and Technologies in Support of Spatially and Spectrally Flexible Optical Networking," *IEEE/OSA Journal of Optical Communications and Networking*, 9, 1, 1-26 (2017).

[34] M. Blau, D.M. Maron, "Wavelength Demultiplexer Design Operating over Multiple Spatial Modes of a Rectangular Waveguide," IEEE Journal of Selected Topics in Quantum Electronics, 26, 4, 4400111-4400 (2020).

[35] R. Ryf, N.K. Fontaine, J. Dunayevsky, D. Sinefeld, M. Blau, M. Montoliu, S. Randel, C. Liu, B. Ercan, M. Esmaeelpour, S. Chandrasekhar, A.H. Gnauck, S.G. Leon-Saval, J. Bland-Hawthorn, J.R. Salazar-Gil, Y. Sun, L. Gruner-Nielsen, R. Lingle Jr., D.M. Maron, "Wavelength-Selective Switch for Few-Mode Fiber Transmission," *in Proc. European Conf. optical Communication (ECOC),* 2013, paper PD1.C.4.

[36] D.M. Maron, J. Dunayevsky, D. Sinefeld, M. Blau, R. Ryf, N.K. Fontaine, M. Montoliu, S. Randel, C. Liu, B. Ercan, M. Esmaeelpour, S. Chandrasekhar, A.H. Gnauck, S.G. Leon-Saval, J. Bland-Hawthorn, J.R. Salazar-Gil, Y. Sun, L. Gruner-Nielsen, R. Lingle Jr., "Wavleength-selective switch with direct few mode fiber integration," Optics Express, 23, 5, 5723-5737 (2015).

[37] S. Mumtaz, R.J. Essiambre, G.P. Agrawal, "Nonlinear Propagation in Multimode and Multicore Fibers: Generalization of the Manakov Equations," Journal of Lightwave Technology, 31, 3, 398-406 (2013).

[38] A. Mecozzi, C. Antonelli, M. Shtaif "Nonlinear propagation in multi-mode fiber in the strong coupling regime," Opt. Express, 20, 11673-11678 (2012).

[39] G. Rademacher, K. Petermann "Nonlinear Gaussian Noise Model for Multimode Fibers With Space-Division Multiplexing," Journal of Lightwave Technology, 34, 9, 2280-2287 (2016).

[40] F. Arpanaei, N. Ardalani, H. Beyranvand, B. Shariati "QoT-aware performance evaluation of spectrally–spatially flexible optical networks over FM-MCFs," Journal of Optical Communications and Networking 12, 8, 288-300 (2020).

[41] H. Liu, H. Wen et al., "Reducing group delay spread in a 9-LP mode FMF using uniform long-period grating," *Proc. OFC 2017*, paper Tu2J.5 (2017)

[42] S. Randel et al., "6 × 56-Gb/s mode-division multiplexed transmission over 33-km few-mode fiber enabled by 6 × 6 MIMO equalization," *Opt. Express*, vol. 19, no. 17, pp. 16697–16707, 2011.

[43] https://metro-haul.eu/

[44] R. Muñoz *et al.*, "SDN control of sliceable multidimensional (spectral and spatial) transceivers with YANG/NETCONF," in *IEEE/OSA Journal of Optical Communications and Networking*, vol. 11, no. 2, pp. A123-A133, Feb. 2019

[45] N. Sambo et al., "Provisioning in Multi-Band Optical Networks," in Journal of Lightwave Technology, vol. 38, no. 9, pp. 2598-2605, 1 May1, 2020, doi: 10.1109/JLT.2020.2983227.